Research article

Two different coordination modes of the Schiff base derived from ortho-vanillin and 2-(2-aminomethyl)pyridine in a mononuclear uranyl complex

Sokratis T. Tsantis [a,b,***], Zoi G. Lada [b], Demetrios I. Tzimopoulos [c], Vlasoula Bekiari [d], Vassilis Psycharis [e], Catherine P. Raptopoulou [e,**], Spyros P. Perlepes [a,b,*]

[a] *Department of Chemistry, University of Patras, 26504 Patras, Greece*
[b] *Institute of Chemical Engineering Sciences, Foundation for Research and Technology-Hellas (Forth/ICE-HT), Platani, P.O. Box 1414, 26504 Patras, Greece*
[c] *Department of Chemistry, Aristotle University of Thessaloniki, 54124 Thessaloniki, Greece*
[d] *Department of Crop Science, University of Patras, 30200 Messolonghi, Greece*
[e] *Institute of Nanoscience and Nanotechnology, NCSR "Demokritos", 15310 Aghia Paraskevi Attikis, Greece*

ABSTRACT

This work describes the reaction of the potentially tetradentate Schiff-base ligand *N*-(2-pyridylmethy)-3-methoxysalicylaldimine (HL) with $UO_2(O_2CMe)_2 \cdot 2H_2O$ and $UO_2(NO_3)_2 \cdot 6H_2O$ in MeOH in the absence or presence of an external base, respectively. The product from these reactions is the mononuclear complex $[UO_2(L)_2]$ (1). Its structure has been determined by single-crystal, X-ray crystallography. The anionic ligand adopts two different coordination modes (1.1011, 1.1010; Harris notation) in the complex. The new compound was fully characterized by solid-state (IR, Raman and Photoluminescence spectroscopies) and solution (UV-Vis and ^{1}H NMR spectra, conductivity measurements) techniques.

1. Introduction

Uranium is a controversial element in the Periodic Table. The reason is the discussion about its use and the relevant consequences. A secondary reason is the fact that it sometimes behaves like lanthanoids but others more like a transition metal [1]. Because of these facts, uranium appears something of a ''Mr. Hyde and Dr. Jekyll character''. The 5f orbitals are well outside the atomic core into the valence region. Thus, the 5f orbitals have a better overlap with the frontier orbitals of the ligands' donor atoms, and this results in increased covalency compared to the 4f orbitals which are considered as more inner orbitals. This radial extension of the 5f orbitals, as well as relativistic effects, are responsible for the variety of oxidation states of uranium (from +II to + VI) [1,2]. Compounds in the oxidation state + IV and +VI are the most common ones.

Hexavalent uranium, as the linear thermodynamically stable *trans*-oxidouranium cation (*trans*-$\{U^{VI}O_2\}^{2+}$ or uranyl ion), dominates the chemistry of this metal. There has been a remarkable growth of interest in the chemistry of the uranyl cation in the last 10 years or so for many

reasons including: (i) topics of metallosupramolecular chemistry [3]; (ii) the oxido reactivity in the uranyl ion [4]; (iii) the development of anionic uranyl-organic materials with large porosity for efficient removal of the radiotoxic $^{127}Cs^+$ ions [5]; (iv) the $\{UO_2\}^{2+}$ uptake by proteins (both artificial and natural) [6]; (v) the chemistry of uranyl-peroxide complexes [7]; (vi) theoretical studies concerning the mechanism of uranyl transport and chemical toxicity *in vivo* [8]; and most importantly (vii) the selective complexation and separation of this metal ion from seawater, environmental and biological samples, and acid media during various steps in nuclear technology [9, 10, 11, 12, 13, 14]. In all those (and other) aspects, the appropriate choice of polydentate organic ligands for uranyl coordination is of paramount importance.

A frequently used class of ligands for $\{UO_2\}^{2+}$ complexation consists of Schiff bases, which were first synthesized by Hugo Schiff in 1864 and contain one or more azomethine (-HC = N-) or imine (>C=N-) groups. Schiff-base ligands are central ''players'' in the development of modern coordination chemistry and their metal complexes are associated with many research areas, including molecular magnetism, multifunctional

* Corresponding author.
** Corresponding author.
*** Corresponding author.

molecular materials, compounds with non-linear optical properties, energetic materials, sensors, bioinorganic and medicinal chemistry, heterogenous and homogenous catalysis, and multielectron redox chemistry [15, 16, 17, 18, 19, 20, 21, 22, 23, 24]. The study of uranyl complexes with Schiff bases as ligands is an important research topic in coordination chemistry. Aspects of interest involve: (a) the employment of the uranyl cation as an excellent template agent for condensation of diketones/dialdehydes and diamines leading to complexes possessing macrocyclic Schiff bases as ligands [25]; (b) the behaviour of neutral uranyl complexes with polydentate chelating Schiff bases to act as anion, e.g. $H_2PO_4^-$, receptors [26]; (c) the efficiency of uranyl/Schiff-base complexes to behave as homogenous catalysts, e.g. for 1,4-thiol addition reactions [27]; (d) the use of such complexes in separation processes associated with nuclear fuel processing and nuclear waste management [28, 29, 30]; (e) the utility of Schiff bases in the reduction and reactivity (functionalization) chemistry of $\{U^{VI}O_2\}^{2+}$ [31]; and (f) theoretical studies on complexes of $\{U^{VI}O_2\}^{2+}$ with Schiff-base molecules and anions as ligands [32].

This work describes the reactions of two uranyl sources (namely uranyl nitrate and uranyl acetate) and the *potentially* tetradentate Schiff base *N*-(2-pyridylmethyl)-3-methoxysalicylaldimine [another name is 2-methoxy-6-(2-pyridylmethyliminomethyl)phenol], abbreviated as HL here; the unique product of these reactions has been fully characterized. The structural formula of the free ligand is illustrated in Scheme 1. The coordination chemistry of HL or/and L$^-$ is poorly investigated and only few complexes with other metal ions have been structurally characterized [33, 34, 35, 36, 37, 38, 39, 40]. This study is in the frame of the intense interest of our groups in several aspects of actinoid (5f) chemistry, with [41, 42, 43] or without [44, 45, 46] Schiff-base ligands.

2. Experimental

2.1. Materials and methods

All experimental manipulations were carried out in the normal laboratory atmosphere using materials (reagents, solvents) as purchased from chemical companies (Alfa Aesar, Sigma-Aldrich); deionized water was produced in-house. The free ligand HL (Scheme 1) was synthesized by the typical 1:1 reaction between 3-methoxy-salicylaldehyde (*o*-vanillin) and 2-(2-aminomethyl)pyridine in EtOH following the procedure described in the literature [33] in a 70% yield (63% reported in ref. [33]). The purity of the yellow solid was confirmed by determination of the melting point (found 102–103 °C, reported 104 °C), and IR and ^{1}H NMR spectroscopies [33]. *Warning*: Although the depleted uranium used in the experiments has a very long half-life, all the precautions for working with radioactive materials must be strictly followed; the reactions were carried out in a fume hood which contains α- and β-counting equipment. In addition to the radioactive uranium hazards, $\{UO_2\}^{2+}$ compounds should be handled with care (use masks and gloves) because they are toxic.

Microanalyses for C, H and N were performed by the Central Laboratory of Instrumental Analysis of the University of Patras using a Carlo-Erba, model EA1108 analyzer. FT-IR spectra in the 4000-400 cm^{-1} were
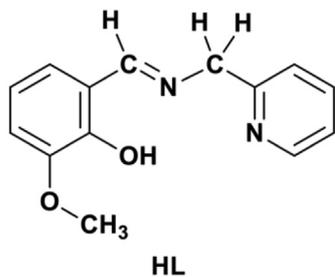
run using a Perkin-Elmer 16PC spectrometer, with samples prepared in the form of KBr pellets under pressure. For the Raman measurements, the T64000 Horiba-Jobin Yvon micro-Raman setup was used. The excitation wavelength was 632.8 nm emitted from a He-Ne laser (Optronics Technologies SA, model HLA-20P, 20mW). The laser power on the samples was 1 mW. The photobleaching of the samples for 30 min, prior to the Raman measurements, was crucial for eliminating or minimizing the overlapping fluorescence effect. The backscattered radiation was collected from a single configuration of the monochromator after passing through a suitable edge filter (LP02-633RU-25, laser2000 Ltd., Huntigdon, Cambridgeshire, UK). The calibration of the instrument was performed *via* the Raman peak position of silicon at 520.5 cm^{-1}. The spectral resolution was less than 5 cm^{-1}. ^{1}H NMR spectra were recorded on a Bruker Avance DPX spectrometer at a resonance frequency of 400.13 MHz; the signal of the solvent (d$_6$-DMSO) was used as reference. Conductivity experiments were carried out at 25 ± 0.5 °C in DMSO with a Metrohm-Herisau E-527 bridge and a cell which has a standard constant; solution concentration was ~10^{-3} M. The UV-VIS spectrum of the complex in DMSO (99%) was recorded in the region 250–800 nm using a Hitachi-U300 spectrometer. Solid state and solution room-temperature photoluminescence studies were performed using a Cary Eclipse fluorescent spectrometer.

2.2. Preparation of the complex [UO$_2$(L)$_2$] (1) and characterization data

2.2.1. Method A

A yellow solution of HL (0.048 g, 0.20 mmol) in MeOH (10 mL) was added to a stirred yellow solution of UO$_2$(O$_2$CMe)$_2$·2H$_2$O (0.043 g, 0.10 mmol) in the same solvent (15 mL). A bordeaux solid was immediately precipitated, the reaction mixture was stirred for a further 15 min and the powder was isolated by filtration. The solid was dissolved in a warm solvent mixture comprising EtOH (3 mL) and CH$_2$Cl$_2$ (12 mL) giving an orange-red solution. The reaction solution was carefully layered with Et$_2$O (5 mL) and X-ray quality bordeaux crystals of the product were grown within a period of 5 d. The crystals were collected by filtration, washed with Et$_2$O (3 × 1 mL) and dried in air. Typical yields were in the range 65–70%. Anal. Calc. for C$_{28}$H$_{26}$N$_4$O$_6$U (F.Wt. = 752.56): C, 44.69; H, 3.49; N, 7.45 %. Found: C, 45.18; H, 3.38; N, 7.41%. IR (KBr, cm^{-1}): 3444 wb, 3074w, 2998w, 2930w, 2830w, 1634s, 1614s, 1572w, 1554m, 1482sh, 1468s, 1441s, 1434sh, 1398m, 1350w, 1302s, 1250s, 1222s, 1190w, 1168w, 1106w, 1080m, 1046m, 1018w, 996w, 972w, 952w, 890s, 854m, 784sh, 772sh, 746s, 652sh, 642w, 610w, 580w, 544w, 494w, 420w, 404w. Raman (1900-100 cm^{-1}): 1634w, 1597w, 1553w, 1467m, 1445m, 1346m, 1329sh, 1312m, 1223wb, 1103w, 1084w, 1055w, 1023w, 997w, 862m, 801s, 642w, 547wb, 499w, 422w, 321wb, 299w, 247w, 240w, 203wb, 175w, 159w, 126w. The IR and Raman spectra of the bordeaux powder and a batch of the crystals were identical. ^{1}H NMR (d$_6$-DMSO, δ/ppm): 9.58 (s, 1H), 7.88 (dd, 1H), 7.72 (d, 1H) 7.57 (d, 1H) 7.31–7.26 (mt, 2H), 6.69 (t, 2H), 3.96 (s, 2H), 3.35 (s, 3H), 2.62 (s, 15H). UV/VIS (DMSO, λ/nm): 275, 353, 409, 485. Λ_M (DMSO, 10^{-3} M, 25 °C) = 5 S cm^2 mol^{-1}. The solid complex emits light at 533, 593 and 651 nm upon excitation at 404 or 436 nm.

2.2.2. Method B

A yellow solution of HL (0.048 g, 0.20 mmol) and Et$_3$N (28 μL, 0.20 mmol) in MeOH (10 mL) was added to a stirred yellow solution of UO$_2$(NO$_3$)$_2$·6H$_2$O (0.050 g, 0.10 mmol) in the same solvent (12 mL). Upon mixing, a bordeaux solid was precipitated. The reaction mixture was stirred for a further 10 min and the powder was isolated by filtration. The solid was dissolved in a warm solvent mixture comprising EtOH (3 mL) and CH$_2$Cl$_2$ (12 mL). The orange-red solution obtained was carefully layered with Et$_2$O (5 mL) and low quality bordeaux crystals were collected by filtration, washed with Et$_2$O (3 × 1 mL) and dried in air. The yield was 42%. Anal. Calcd. for C$_{28}$H$_{26}$N$_4$O$_6$U (F.Wt. = 752.56): C, 44.69; H, 3.49; N, 7.45 %. Found: C, 44.81; H, 3.60; N, 7.27 %. The sample had identical IR, Raman and ^{1}H NMR spectra with the solid isolated using the

Scheme 1. The structural formula and abbreviation of the *potentially* tetradentate Schiff base *N*-(2-pyridylmethyl)-3-methoxysalicylaldimine [or 2-methoxy-6-(2-pyridylmethyliminomethyl)phenol].

method A. Λ_M (DMSO, 10^{-3} M, 25 °C) = 2 S cm^2 mol^{-1}. The IR spectra of the powder and the crystals were identical.

2.3. Single-crystal X-ray crystallography

A crystal of **1** obtained by method A was taken from the mother liquor and immediately cooled at 170 K. Diffraction data were collected on a Rigaku R-AXIS Image Plate diffractometer using graphite-monochromated Cu Kα radiation. With the use of this radiation (and not Mo Kα) the absorption factor takes a value of 18.05 mm^{-1}; the average size of the measured crystal was 0.27 mm. The product of the two quantities is ~5. This value is above 3 and thus a numerical absorption correction was applied resulting in a very good data set with few, not serious alerts in the checkcif file. Data collection (ω-scans) and processing (cell refinement, data reduction and numerical absorption correction) were performed using the CrystalClear program package [47].

The structure was solved by direct methods using SHELXS, ver. 2013/1 [48], and refined by full-matrix least-squares techniques on F^2 with SHELXL ver. 2014/6 [49]. All H atoms were introduced at calculated positions as riding on their corresponding bonded atoms. All non-H atoms were refined anisotropically. Structural plots were drawn using the Diamond 3 program package [50]. The crystallographic details are listed in Table 1. CCDC 2165160 contains the supplementary data for this paper. These data can be obtained free of charge from the Cambridge Crystallographic Data Center via www.ccdc.cam.ac.uk/data_request/cif; E-mail: deposit@ccdc.cam.ac.uk.
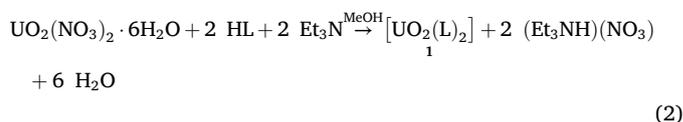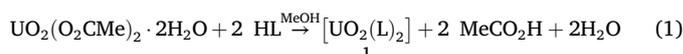
3. Results and discussion

3.1. Synthetic comments

In the present work, we have studied the reactions between the Schiff base-ligand HL and uranyl sources; uranyl complexes with this ligand did not exist in the literature. Many synthetic parameters were explored involving the uranyl source (chloride, nitrate, acetate), the solvent, the temperature, the pressure (i.e. solvothermal conditions), the presence/absence of external bases (Et$_3$N, NaOMe, Me$_4$NOH·5H$_2$O), the absence/presence of bulky countercations or counteranions (to investigate the possibility of existence of anionic or cationic complexes, respectively), the reaction time and the crystallization techniques, before arriving at the optimized conditions described in section 2. It seems that complex [UO$_2$(L)$_2$] (**1**) is the only product in all the cases. The reactions described in paragraphs 2.2.1 and 2.2.2 are represented by Eqs. (1) and (2), respectively.

$$\text{UO}_2(\text{O}_2\text{CMe})_2 \cdot 2\text{H}_2\text{O} + 2 \ \text{HL} \xrightarrow{\text{MeOH}} \big[\text{UO}_2(\text{L})_2\big] + 2 \ \text{MeCO}_2\text{H} + 2\text{H}_2\text{O} \quad (1)$$
$$\qquad\qquad\qquad\qquad\qquad\qquad\qquad\mathbf{1}$$

$$\text{UO}_2(\text{NO}_3)_2 \cdot 6\text{H}_2\text{O} + 2 \ \text{HL} + 2 \ \text{Et}_3\text{N} \xrightarrow{\text{MeOH}} \big[\text{UO}_2(\text{L})_2\big] + 2 \ (\text{Et}_3\text{NH})(\text{NO}_3)$$
$$\qquad\qquad\qquad\qquad\qquad\qquad\qquad\qquad\qquad\mathbf{1}$$
$$+ \ 6 \ \text{H}_2\text{O}$$
$$\qquad\qquad\qquad\qquad\qquad\qquad\qquad\qquad\qquad\qquad (2)$$

Two points deserve further comments: (i) The use of the uranyl acetate starting material gives higher yields and crystals of better quality; and (ii) the {UO$_2$}$^{2+}$:HL reaction ratio does not affect the product identity since the 1:1 UO$_2$(O$_2$CMe)$_2$·2H$_2$O/HL and 1:1:1 UO$_2$(NO$_3$)$_2$·6H$_2$O/HL/Et$_3$N reaction systems lead again to compound **1** (microanalytical and IR evidence), suggesting that this complex is the thermodynamically preferred product from the general {UO$_2$}$^{2+}$/HL system.

3.2. Description of structure

Selected bond distances and angles, and parameters for H-bonding interactions are listed in Tables 2 and 3, respectively. Structural plots are shown in Figures 1, 2, and 3.

Compound **1** crystallizes in the monoclinic space group $P2_1/c$ and the asymmetric unit contains one [UO$_2$(L)$_2$] molecule. The U^{VI} atom is surrounded by four oxygen and three nitrogen atoms in a distorted pentagonal bipyramidal geometry. The two 1.1 uranyl oxygen atoms (O5, O6) occupy the axial positions, as expected. One oxygen (O3) and two nitrogen (N3, N4) atoms from a 1.1011 (Harris notation [51]) L$^-$ ligand, and one oxygen (O2) and one nitrogen (N1) atoms from a 1.1010 L$^-$

Table 1. Crystallographic data for compound **1**.

Parameter	
Formula	C$_{28}$H$_{26}$UN$_4$O$_6$
Formula weight	752.56
Crystal system	Monoclinic
Space group	$P2_1/c$
Color	Bordeaux
Crystal size (mm)	0.21 × 0.23 × 0.38
Crystal habit	Prismatic
a (Å)	11.849 (2)
b (Å)	10.8039 (2)
c (Å)	20.9278 (4)
β (°)	103.626 (1)
Volume (Å^3)	2593.99 (8)
Z	4
Temperature (K)	170
Radiation (Å)/$2\theta_{max}$	Cu Kα (1.54178/134.0)
ρ_{calcd} (g cm^{-3})	1.927
μ (mm^{-1})	18.05
Measured, unique (R_{int}) and observed [$I > 2\sigma(I)$] reflections	34909, 4454 (0.064) and 4401
No. of parameters	354
R_1, wR_2 [$I > 2\sigma(I)$]^a	0.0299, 0.0720
R_1, wR_2 (all data)^a	0.0301, 0.0722
Goodness-of-fit (on F^2)	1.12
$\Delta\rho_{max}/\Delta\rho_{min}$ (e Å^{-3})	1.78, -2.02

^{a} $R_1 = \Sigma(|F_o|-|F_c|)/\Sigma(|F_o|)$, $wR_2 = \{\Sigma[w \ (F_o^2-F_c^2)^2]/\Sigma[w \ (F_o^2)^2]\}^{1/2}$, $w = 1/[\sigma^2(F_o^2)+(\alpha P)^2 + bP]$ where $P = [\max \ (F_o^2, \ 0)+2F_c^2]/3$, $\alpha = 0.0196$ and $b = 17.2310$.

Table 2. Selected bond lengths (Å) and angles (°) for complex **1**.

Bond lengths			
U1-O5	1.794(4)	C9-C10	1.512(9)
U1-O6	1.791(4)	C9-N1	1.477(8)
U1-O2	2.229(4)	C8-N1	1.291(7)
U1-O3	2.261(4)	C2-O1	1.370(7)
U1-N1	2.552(4)	C16-O4	1.376(7)
U1-N3	2.598(5)	C22-N4	1.277(8)
U1-N4	2.546(5)	C23-N4	1.477(8)
Bond lengths			
O5-U1-O6	177.2(2)	O2-U1-O3	154.1(1)
O5-U1-O2	90.7(2)	O2-U1-N1	71.2(1)
O5-U1-O3	88.5(1)	O2-U1-N3	73.9(1)
O5-U1-N1	96.6(2)	O2-U1-N4	136.1(2)
O5-U1-N3	86.9(2)	O3-U1-N1	83.2(1)
O5-U1-N4	93.4(2)	O3-U1-N3	131.8(1)
O6-U1-O2	89.7(2)	O3-U1-N4	69.8(2)
O6-U1-O3	92.1(2)	N1-U1-N3	144.9(2)
O6-U1-N1	85.7(2)	N1-U1-N4	150.9(1)
O6-U1-N3	91.0(2)	N3-U1-N4	62.7(2)
O6-U1-N4	84.7(2)	C8-N1-C9	115.2(5)
		C6-C8-N1	127.7(5)

Table 3. H-bonding interactions in the crystal structure of complex 1.

D-H⋯A	D⋯A (Å)	H⋯A (Å)	D-H⋯A (°)	Symmetry of A
C9-H$_A$(C9)⋯O3[a]	3.296(7)	2.56	130.7(4)	*x, y, z*
C9-H$_A$(C9)⋯O4[a]	3.576(8)	2.61	165.2(4)	*x, y, z*
C28-H(C28)⋯O1[a]	2.977(7)	2.47	113.2(2)	*x, y, z*
C28-H(C28)⋯O2[a]	2.921(7)	2.35	117.8(4)	*x, y, z*
C8-H(C8)⋯O6′[b]	3.512(6)	2.69	145.1(4)	*-x+1, -y, -z+2*
C17-H(C17)⋯O5″[b]	3.544(8)	2.60	173.8(5)	*-x+2, y-1/2, z+5/2*

[a] Intramolecular H bonds. [b]Intermolecular H bonds. Abbreviations: D = Donor; A = acceptor.
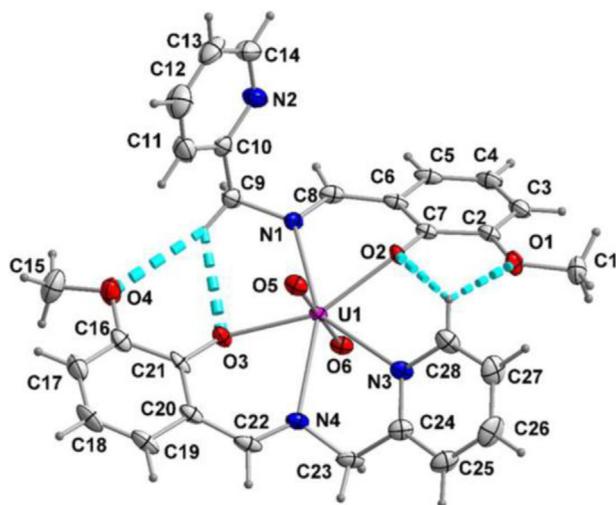
Figure 1. Fully labelled ORTEP plot of the [UO$_2$(L)$_2$] molecule that is present in the structure of **1**. The thermal ellipsoids are presented at the 50% probability level. The thick dashed cyan lines indicate bifurcated H bonds of the C-H⋯O type (Table 3).
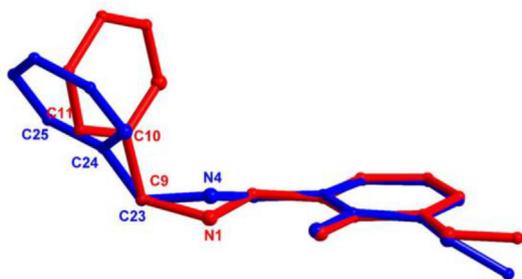
Figure 2. The two L⁻ ligands of complex 1 presented in the overlay mode. The N1-, N2- and N4-, N3- containing ligands are represented by red and blue colors, respectively.

group define the equatorial plane; the pyridyl nitrogen (N2) of the latter ligand remains uncoordinated. Thus, the two L⁻ ligands in **1** adopt two different ligation modes (1.1011 and 1.1010; Scheme 2). A consequence of the different modes is the angle between the two aromatic rings of each ligand; this is 88.3(2)° for the bidentate 1.1010 ligand (i.e., the two rings are nearly perpendicular) and 53.3(2)° in the case of the tridentate 1.1011 ligand. The difference is further reflected in the overlay diagram, shown in Figure 2. The two pyridyl ends of the L⁻ ligands clearly present different orientations, as it is also revealed by the torsion angles N1-C9-C10-C11 and N4-C23-C24-C25 which take the values -114.9(6) and 150.2(6)°, respectively. There are two bifurcated, non-classical intramolecular H bonds (Figure 1, Table 3). In one of them, the donor

is the pyridyl carbon atom C28 of the tridentate L⁻ ligand, and the acceptors are the coordinated phenolato oxygen atom (O2) and the ''free'' methoxy oxygen atom (O1) both from the bidentate ligand. In the second intramolecular H bond, the donor is the methylene carbon atom C9 of the bidentate ligand, and the acceptors are the coordinated phenolato oxygen atom (O3) and the ''free'' methoxy oxygen atom (O4) both from the tridentate ligand.

The U=O [5,6] bonds (~1.79 Å) are slightly elongated compared to those of typical *trans*-{U^{VI}O$_2$}$^{2+}$ complexes [4,41,42,44,45], while the O=U=O unit is slightly bent (~177°); the reason for these experimental facts will be discussed below. The C8-N1 and C22-N4 bond lengths are 1.291(7) and 1.277(8) Å, respectively, suggesting double carbon-nitrogen bonds indicative of Schiff-base linkages. On the other hand, the single carbon-nitrogen bond character of the C$_{methylene}$-N$_{imino}$ distances is confirmed by their bond lengths which are both 1.477(8) Å.

The bond angles between the neighboring atoms in the equatorial plane are in the range 62.7(2)-83.2(1)°. These angles deviate from the ideal value of 72° for the perfect pentagonal bipyramid indicating a distorted geometry. This distortion is primarily a consequence of the small bite angles due to the formation of the N4C23C24N3U1 chelating ring [N3-U1-N4 = 62.7(2) °]. Furthermore, the five equatorial donor atoms deviate from their best mean plane by 0.032(O2), 0.113(N1), 0.173(O3), 0.172(N4) and 0.079(N3) Å.

Further to the intramolecular H bonds described above, intermolecular H bonds are also present in the crystal structure of **1** (Figure 3, Table 3). Neighboring centrosymmetrically-related molecules form dimers through C8-H(C8)⋯O6′ and C8′-H(C8′)⋯O6 H-bonding interactions (symmetry codes: -x+1, -y, -z+2). The ''dimers'' interact further through C17-H(C17)⋯O5″ (and symmetry related) H bonds forming layers parallel to (10–2) planes (symmetry code: -x+2, y-1/2, z+5/2). These two intermolecular H bonds, which involve the uranyl oxo atoms (the so-named O$_{yl}$ atoms [52]), are most probably responsible for the elongation of the U=O$_{yl}$ bond lengths and the moderate bent of the *trans*-{U^{VI}O$_2$}$^{2+}$ unit [4,31,52, 53, 54]. Other reasons for this bending might be unfavorable steric interactions between the equatorial donor atoms and the uranyl oxo groups as revealed by the ''large'' O3-U1-N1 bond angle (which deviates from the ideal of 72°) [53], the relatively strong σ-donating abilities of the equatorial L⁻ ligands [53] and π donation from the equatorial ligands into the 6d and 5f orbitals of U(VI) [54].

Complex **1** is a new member of a small family of metal complexes possessing the L⁻ ligand (there are no structurally characterized complexes of the neutral HL ligand). For convenience, we have listed all these complexes in Table 4 along with the coordination modes of L⁻; the latter are drawn in Scheme 2. Perusal of Table 4 reveals that the ligation mode 1.1010 has been observed for the first time in the uranyl complex of the present work, while **1** is the first complex in which two different coordination modes of L⁻ co-exist.

3.3. Spectroscopic characterization of **1** in brief

Spectroscopic data are shown in Figures 4, 5, and 6 and S1. The two strong bands at 1634 and 1614 cm⁻¹ in the IR spectrum of **1** are attributed to the ν(C=N) vibration of the Schiff-base group [33]. The appearance of two bands in the spectrum of **1** is probably a consequence of the presence of two different L⁻ ligands in the complex. The corresponding Raman peak is located at 1634 cm⁻¹. The IR band of strong intensity in the spectrum of the complex at 890 cm⁻¹ is assigned [42,44, 55] to the IR-active antisymmetric stretch of the *trans*-{U^{VI}O$_2$}$^{2+}$ group (ν_3). The strong Raman peak at 801 cm⁻¹ is due to the corresponding symmetric stretching vibration (ν_1) [53-55]. It is well documented that the uranyl cation features three characteristic vibrational modes: a symmetric stretching vibration (ν_1, 850-880 cm⁻¹, Raman active), a bending vibration (ν_2, ~200 cm⁻¹, IR-active, well below the detection limits of most IR spectrometers) and an asymmetric stretching vibration (ν_3, 920-960 cm⁻¹, IR-active). The red shift of both the IR band and the
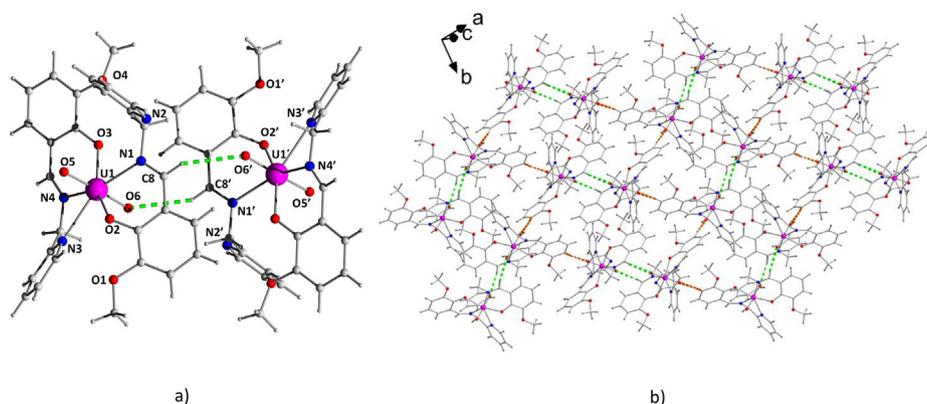
Figure 3. (a) A H-bonded dimer in the crystal structure of complex **1** (symmetry code: -*x*+1, -*y*, -*z*+2). (b) Layers of dimers parallel to the (10–2) planes. Dashed light green and orange lines represent the C8-H(C8)…O6′ and C17-H(C17)…O5″ H bonds, respectively. See Table 3 for metric parameters and symmetry operations, and the text for details.
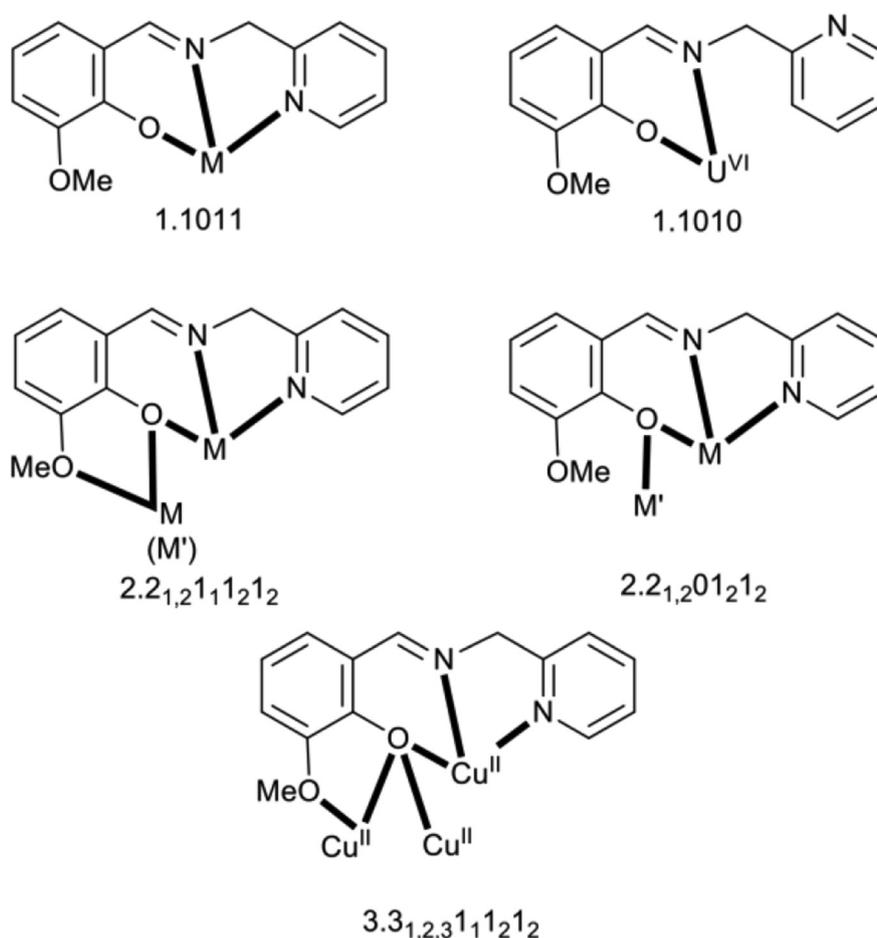
Scheme 2. The to-date crystallographically confirmed coordination modes of L⁻ using the Harris notation [51]. In the 1.1011 mode, M is Cu^{II}, Zn^{II} and Pd^{II}. In the 2.2$_{1,2}$1$_1$1$_2$1$_2$ mode, either M = Cd^{II} or M = Zn^{II} and M′ = Ln^{III} (Sm^{III}, Eu^{III}, Gd^{III}, Tb^{III}). In the 2.2$_{1,2}$01$_2$1$_2$ mode, M = Ni^{II} and M′ = Ln^{III} (Sm^{III}, Eu^{III}). Coordination bonds are drawn with bold lines.

Raman peak in **1**, compared with those of typical uranyl complexes, is ascribed [42,53,54] to the weakening of the axial uranium(VI)-oxo bonds (due to the negative charge in the equatorial plane and the participation of the axial atoms in H bonds) and to the slight bending of the *trans*-OU^{VI}O unit (due to H-bonding interactions involving the oxo groups, the σ-donating ability of the L⁻ ligands, the π-donation from these ligands and the steric interactions involving the equatorial donor atoms) [52-54].

The old and simplified empirical equation $0.933 \times \nu_3 = \nu_1$ [56], which has been derived for compounds containing strictly linear *trans*-{U^{VI}O$_2$}$^{2+}$ groups, does not apply for **1** in accordance with the deviation (albeit small) from linearity.

The ^{1}H NMR spectrum of **1** in d$_6$-DMSO is simple and does not change with time, probably suggesting the equivalence of the two ligands L⁻ and the presence of one species in solution. The spectrum is different from

Table 4. Up-to-date structurally characterized homo- and heterometallic complexes containing the organic ligand L⁻. The ligation modes are abbreviated using the Harris notation [51].

Complex[a,b]	Ligation mode of L[-d]	Ref.
[Cu^{II}X(L)]	1.1011	[33]
[Cu^{II}$_4$(L)$_4$](ClO$_4$)$_4$[c]	$3.3_{1,2,3}1_11_21_2$	[34]
[Cu^{II}(N$_3$)(L)]	1.1011	[35]
[Pd^{II}(O$_2$CMe)(L)]	1.1011	[36]
[ZnCl(L)]	1.1011	[37]
[Cu(NCS)(L)(DMF)]	1.1011	[40]
[Cd$_2$(NCS)$_2$(L)$_2$]	$2.2_{1,2}1_11_21_2$	[39]
[ZnLn(NO$_3$)$_2$(L)$_2$][e]	$2.2_{1,2}1_11_21_2$	[38]
[NiSm(NO$_3$)$_3$(L)$_2$(H$_2$O)$_2$][e]	$2.2_{1,2}01_21_2$	[38]
[NiEu(NO$_3$)$_3$(L)$_2$(H$_2$O)][e]	$2.2_{1,2}01_21_2$	[38]
[UO$_2$(L)$_2$] (1)	$1.1011, 1.1010$	this work

Abbreviations: DMF = N,N-dimethylformamide; Ln = Sm, Eu, Gd, Tb; X = Cl, Br.
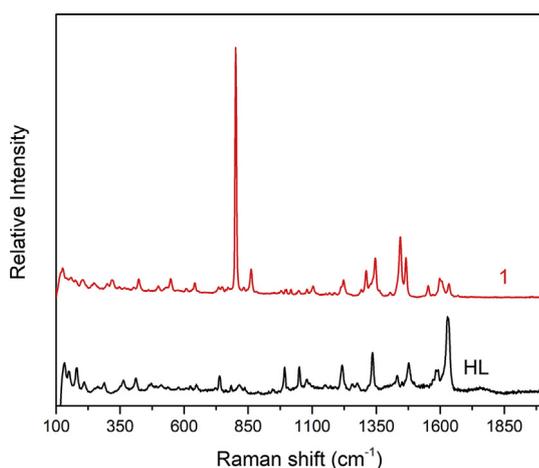
[a] There are no characterized metal complexes with the neutral HL ligand.

[b] Lattice solvent molecules have been omitted.

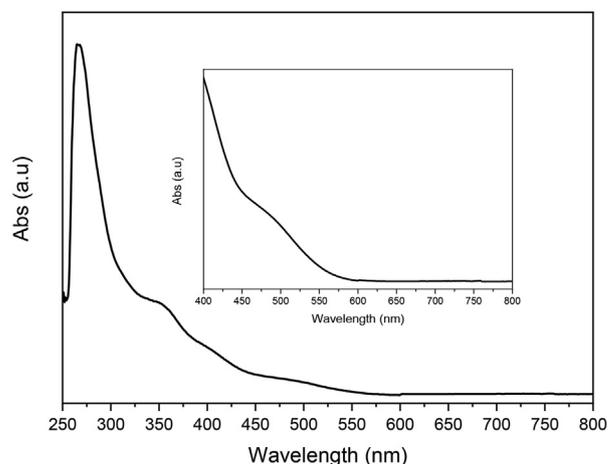[c] The molecule contains a heterocubane $\{Cu^{II}_4(\mu_3\text{-}OR)_4\}^{4+}$ core, where $RO^- = L^-$.

[d] See also Scheme 2.

[e] The subscript 1 refers to the Ln^{III} ion and the subscript 2 refers to the transition metal ion.

Figure 5. The UV/VIS spectrum of complex **1** in DMSO. The VIS spectrum of a more concentrated solution is shown in the inset.

Figure 6. Solid-state, room-temperature excitation (maximum emissions at 533, 593 and 651 nm) (curve 1) and emission (maximum excitations at 404 or 436 nm) (curve 2) of complex **1**.
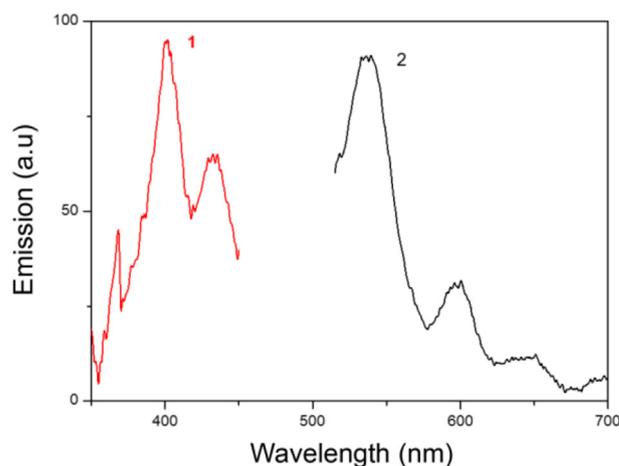

Figure 4. The Raman spectrum of the free ligand HL and complex **1** in the 1900-100 cm⁻¹ region.

that of the free ligand HL in MeOD [33]. This fact and the nonappearance of -OH signals in the spectrum both confirm the existence of deprotonated L⁻ anions in solution; the almost negligible value of molar conductivity of **1** in DMSO (5 S cm² mol⁻¹) implies that the L⁻ ions remain coordinated [57]. The singlet signals at δ values 9.58, 3.96 and 3.35 ppm are assigned to the imine, benzylic (-CH$_2$-) and methoxy (-OCH$_3$) protons, respectively [33]; the integration ratio of these signals is 1:2:3, as expected. The aromatic protons appear in the δ range 7.88–6.69 ppm. The equivalence of the two coordinated L⁻ ions (in the solid state one ligand is bidentate and the other is tridentate) is a strong evidence of the same coordination mode in solution. The non-deshielded nature of the aromatic protons next to the pyridyl nitrogen atoms (at δ 7.88 ppm) make us tentatively propose that the two equivalent L⁻ ligands are O(phenolato), N(imine)-bidentate chelating in solution; an appreciable downfield shift of this signal would be expected in the case of N(pyridyl)-coordination. Thus, the neutral complex species in solution appears to be [UO$_2$(L)$_2$(DMSO)$_x$] (x = 1 or 2). The presence of coordinated DMSO molecule(s) in the complex in solution is further corroborated by the appearance of a singlet signal at δ 2.62 ppm, slightly downfield shifted from the main -CH$_3$ signal of the non-deuterated percentage of the

solvent (at δ 2.50 ppm). It is well established that the dipolar, aprotic solvent DMSO is a strong O-bonded donor to the uranyl ion [58].

The electronic spectrum of the free ligand HL in DMSO shows absorption bands at 280, 331 and 424 nm, the former two being assigned [32-34] to $\pi\rightarrow\pi^*$ transitions of the imine linkage and the aromatic rings, and the latter to the $n\rightarrow\pi^*$ transitions of the pyridyl group. Solutions of **1** in DMSO are red. Spectra of varying concentrations exhibit bands at 275, 353 and 409 nm due to intraligand transitions, which have been somewhat shifted from those of the free HL due to its deprotonation and coordination in the complex [32,33]. Uranyl complexes typically absorb at ~425 nm due to ligand-to-metal charge transfer (LMCT). This band often displays clearly appeared vibronic progressions as, for example, seen in the spectrum of UO$_2$(NO$_3$)$_2$·6H$_2$O [53]. In the solution spectra of **1**, the LMCT transition is hypsochromically shifted by ~60 nm, and a band appears at 485 nm which is not observed in classical uranyl complexes (usually of yellow color). The band at 485 nm gives the red color which has been considered as evidence for the bending of the *trans*-OU^{VI}O group and the weakening of the U^{VI}-O$_{yl}$ bonds, both seen in the structure of **1** [53].

Room-temperature emission spectra of the free ligand HL and compound **1** in the solid state were recorded. Upon maximum excitation at 496 nm, HL exhibits an emission band centered at 550 nm. The same emission band is also observed in a DMSO solution of the free ligand. A

solid sample of the complex also emits light; upon maximum excitations at 404 or 436 nm, broad emission bands with maxima at ~535, ~595 and ~650 nm are recorded (Figure 6). Some uranyl compounds exhibit a characteristic green emission pattern with strong vibronic coupling, leading to a well-resolved five-peak pattern [54,59, 60, 61]. The green emission at ~520 nm arises from ligand-to-metal charge transfer transitions between uranyl $3\sigma_u$, $3\sigma_g$, $2\pi_u$ and $1\pi_g$ and the nonbonding 5f δ_u and φ_u molecular orbitals [54]. The fluorescence of uranyl compounds, first recorded by Brewster in 1833, allowed Stokes to confirm his law in 1852 and played an incidental role in the discovery of radioactivity by Becquerel in 1896 [59]; it is thus of historical value. The emission peaks resolved in the spectrum of **1** are tentatively assigned to the uranyl cation [60,61]; the most intense peak is positioned at 533 nm. The emission pattern is shifted to longer wavelengths relative to the corresponding profile in the spectrum of $UO_2(NO_3)_2 \cdot 6H_2O$, and this difference has been interpreted as arising from the influence of the coordinated deprotonated ligands [60]. An alternative assignment of the 595 nm emission peak is that this is ligand-based; it is red-shifted by ~50 nm relative to the emission of HL, due to the deprotonation and coordination of the ligand [42].

4. Concluding remarks

The important messages of this work-in our opinion-are: (a) The $\{U^{VI}O_2\}^{2+}$/HL reaction system gives one product, namely **1**; this compound is the first structurally characterized 5f-metal complex of HL or L^-. (b) The structure of **1** exhibits some interesting features, i.e., elongation of the *trans* uranium(VI)-oxo bonds through participation of the O_{yl} atoms in intermolecular H bonds, bent of the *trans*-$\{OU^{VI}O\}^{2+}$ unit, a new ligation mode (1.1010) in the coordination chemistry of HL, and the simultaneous presence of one bidentate and one tridentate chelating L^- ligands; and (c) Complex **1** has some exciting spectroscopic characteristics, i.e., the low wavenumber of the $\nu(OU^{VI}O)$ vibrational modes (IR and Raman), a VIS band at 485 nm in solution which gives rise to its red color and an interesting emission pattern; the former features are related to the rather long $U^{VI}-O_{yl}$ bonds and the slight bending of the $\{O_{yl}U^{VI}O_{yl}\}$ unit. Efforts are in progress to study the photocatalytic properties of **1**, and prepare and study uranyl complex(es) with the Schiff base derived from *ortho*-vanillin and 2-(2-aminoethyl)pyridine (i.e., the similar ligand containing two -CH_2- groups instead of one) in order to evaluate the bulkier and more flexible character of the latter ligand in terms of the structural and electronic properties of the product(s).

Declarations

Author contribution statement

Sokratis T. Tsantis: Conceived and designed the experiments; Performed the experiments; Analyzed and interpreted the data.

Zoi G. Lada, Demetrios I. Tzimopoulos, Vlasoula Bekiari: Contributed reagents, materials, analysis tools or data.

Vassilis Psycharis, Catherine P. Raptopoulou: Analyzed and interpreted the data; Contributed reagents, materials, analysis tools or data.

Spyros P. Perlepes: Conceived and designed the experiments; Analyzed and interpreted the data; Wrote the paper.

Data availability statement

Data included in article/supplementary material/referenced in article.

References

[1] S.T. Liddle, The renaissance of non-aqueous uranium chemistry, Angew. Chem. Int. Ed. 54 (2015) 8604–8641 (Angewandte review).

[2] C.E. Housecroft, A.G. Sharpe, Inorganic Chemistry, fifth ed., 1035, Pearson, Harlow, UK, 2018, pp. 1054–1057.

[3] H. Kazama, S. Tsushima, Y. Ikeda, K. Takao, Molecular and crystal structures of uranyl nitrate coordination polymers with double-headed 2-pyrrolidone derivatives, Inorg. Chem. 56 (2017) 13530–13534.

[4] S. Fortier, T.W. Hayton, Oxo ligand functionalization in the uranyl ion (UO_2^{2+}), Coord. Chem. Rev. 254 (2010) 197–214.

[5] J. Ai, F.-Y. Chen, C.-Y. Gao, H.-R. Tian, Q.-J. Pan, Z.-M. Sun, Porous anionic uranyl–organic networks for highly efficient Cs^+ adsorption and investigation of the mechanism, Inorg. Chem. 57 (2018) 4419–4426.

[6] S.O. Odoh, G.D. Bondarevsky, J. Karpus, Q. Cui, C. He, R. Spezia, L. Gagliardi, UO_2^{2+} uptake by proteins: understanding the binding features of the super uranyl binding protein and design of a protein with higher affinity, J. Am. Chem. Soc. 136 (2014) 17484–17494.

[7] H.L. Lobeck, J.K. Isner, P.C. Burns, Transformation of uranyl peroxide studtite, $[(UO_2)(O_2)(H_2O)_2](H_2O)_2$, to soluble nanoscale cage clusters, Inorg. Chem. 58 (2019) 6781–6789.

[8] K.E. Gutowski, V.A. Cocalia, S.T. Griffin, N.J. Bridges, D.A. Dixon, R.D. Rogers, Interactions of 1-methylimidazole with $UO_2(CH_3CO_2)_2$ and $UO_2(NO_3)_2$: structural, spectroscopic, and theoretical evidence for imidazole binding to the uranyl ion, J. Am. Chem. Soc. 129 (2007) 526–536.

[9] C.W. Abney, R.T. Mayes, T. Saito, S. Dai, Materials for the recovery of uranium from seawater, Chem. Rev. 117 (2017) 13935–14013.

[10] A. Leoncini, J. Huskens, W. Verboom, Ligands for f-element extraction used in the nuclear fuel cycle, Chem. Soc. Rev. 46 (2017) 7229–7273.

[11] B.G. Vats, S. Kannan, I.C. Pius, D.M. Noronha, D.K. Maity, M.G.B. Drew, Synthetic, structural, extraction and theoretical studies of uranyl nitrate dithio-diglycolamide compounds, Polyhedron 75 (2014) 81–87.

[12] J. Ding, Z. Yan, L. Feng, F. Zhai, X. Chen, Y. Xu, S. Tang, C. Huang, L. Li, N. Pan, Y. He, Y. Jin, C. Xia, Benzotriazole decorated graphene oxide for efficient removal of U(VI), Environ. Pollut. 253 (2019) 221–230.

[13] T. Sukhbaatar, M. Duvail, T. Dumas, S. Dourdain, G. Arrachart, P.L. Solari, P. Guilbaud, S. Pellet-Rostaing, Probing the existence of uranyl trisulfate structures in the AMEX solvent extraction process, Chem. Commun. 55 (2019) 7583–7586.

[14] X. Wang, X. Dai, C. Shi, J. Wan, M.A. Silver, L. Zhang, L. Chen, X. Yi, B. Chen, D. Zhang, K. Yang, J. Diwu, J. Wang, Y. Xu, R. Zhou, Z. Chai, S. Wang, A 3,2-Hydroxypyridinone-based decorporation agent that removes uranium from bones in vivo, Nat. Commun. 10 (2019) 2570, 13.

[15] X. Liu, J.-R. Hamon, Recent developments in penta-, hexa- and heptadentate Schiff base ligands and their metal complexes, Coord. Chem. Rev. 389 (2019) 94–118.

[16] L. Rigamonti, A. Forni, S. Righetto, A. Pasini, Push–pull unsymmetrical substitution in nickel(II) complexes with tetradentate N_2O_2 Schiff base ligands: synthesis, structures and linear–nonlinear optical studies, Dalton Trans. 48 (2019) 11217–11234.

[17] S. Yamada, Advancement in stereochemical aspects of Schiff base metal complexes, Coord. Chem. Rev. 190–192 (1999) 537–555.

[18] K.C. Gupta, A.K. Sutar, Catalytic activities of Schiff base transition metal complexes, Coord. Chem. Rev. 252 (2008) 1420–1450.

[19] J. Long, Luminescent Schiff-base lanthanide single-molecule magnets: the association between optical and magnetic properties, Front. Chem. 7 (2019) article 63.

[20] C. Camp, V. Guidal, B. Biswas, J. Pécaut, L. Dubois, M. Mazzanti, Multielectron redox chemistry of lanthanide Schiff-base complexes, Chem. Sci. 3 (2012) 2433–2448.

[21] E.C. Constable, Metals and Ligand Reactivity, VCH, Weiheim, Germany, 1996, pp. 72–78, 135-182.

[22] N.C. Anastasiadis, C.M. Granadeiro, N. Klouras, L. Cunha-Silva, C.P. Raptopoulou, V. Psycharis, V. Bekiari, S.S. Balula, A. Escuer, S.P. Perlepes, Dinuclear lanthanide(III) complexes by metal-ion-assisted hydration of di-2-pyridyl ketone azine, Inorg. Chem. 52 (2013) 4145–4147.

[23] K.I. Alexopoulou, A. Terzis, C.P. Raptopoulou, V. Psycharis, A. Escuer, S.P. Perlepes, Ni^{II}_{20} "bowls" from the use of tridentate Schiff bases, Inorg. Chem. 54 (2015) 5615–5617.

[24] N.C. Anastasiadis, C.M. Granadeiro, J. Mayans, C.P. Raptopoulou, V. Bekiari, L. Cunha-Silva, V. Psycharis, A. Escuer, S.S. Balula, K.F. Konidaris, S.P. Perlepes, Multifunctionality in two families of dinuclear lanthanide(III) complexes with a tridentate Schiff-base ligand, Inorg. Chem. 58 (2019) 9581–9585.

[25] O. Costisor, W. Linert, 4f and 5f metal ion directed Schiff condensation, Rev. Inorg. Chem. 24 (2004) 61–95.

[26] D.M. Rudkevich, W. Verboom, Z. Brzozka, M.J. Palys, W.P.R.V. Stauthamer, G.J. van Hummel, S.M. Franken, S. Harkema, J.F.J. Engbersen, D.N. Reinhoudt, Functionalized UO_2 salenes: neutral receptors for anions, J. Am. Chem. Soc. 116 (1994) 4341–4351.

[27] V. Van Axel Castelli, A. Cort Dalla, L. Mandolini, Supramolecular catalysis of 1,4-thiol addition by salophen-uranyl complexes, J. Am. Chem. Soc. 120 (1998) 12688–12689.

[28] S.K. Sahu, V. Chakravortty, Extraction of uranium(VI) with binary mixtures of a quadridentate Schiff base and various neutral donors, J. Radioanal. Nucl. Chem. 227 (1998) 163–165.

[29] C.A. Hawkins, C.G. Bustillos, R. Copping, I. May, M. Nilsson, Investigations of hydrophilic Schiff base ligands for the separation of actinyl and lanthanide cations, NEA/NSC/R 2 (2015) 315–323.

[30] C.A. Hawkins, C.G. Bustillos, R. Copping, B.L. Scott, I. May, M. Nilsson, Challenging conventional f-element separation chemistry-reversing uranyl(VI)/lanthanide(III) solvent extraction selectivity, Chem. Commun. 50 (2014) 8670–8673.

[31] B.E. Cowie, J.M. Purkis, J. Austin, J.B. Love, P.L. Arnold, Thermal and photochemical reduction and functionalization chemistry of the uranyl dication, $[U^{VI}O_2]^{2+}$, Chem. Rev. 119 (2019) 10595–10637.

[32] B.E. Klamm, C.J. Windorff, C. Celis-Barros, M.L. Marsh, T.E. Albrecht-Schmitt, Synthesis, spectroscopy and theoretical details of uranyl Schiff-base coordination complexes, Inorg. Chem. 59 (2020) 23–31.

[33] R. Kannappan, S. Tanase, I. Mutikainen, U. Turpeinen, J. Reedijk, Square-planar copper(II) halide complexes of tridentate ligands with π-π stacking interactions and alternating short and long Cu...Cu distances, Inorg. Chim. Acta. 358 (2005) 383–388.

[34] C. Maxim, T.D. Pasatoiu, V.C. Kravtsov, S. Shova, C.A. Muryn, R.E.P. Winpenny, F. Tuna, M. Andruh, Copper(II) and zinc(II) complexes with Schiff-base ligands derived from salicylaldehyde and 3-methoxysalicylaldehyde: synthesis, crystal structures, magnetic and luminescence properties, Inorg. Chim. Acta. 361 (2008) 3903–3911.

[35] X. Sun, (Azido-κN)[6-methoxy-2-(2-pyridylmethyliminomethyl)phenolato-κ³N,N′,O¹]copper(II), Acta Crystallogr. E64 (2008) m33.

[36] S.A. Patil, C.-M. Weng, P.-C. Huang, F.-E. Hong, Convenient and efficient Suzuki–Miyaura cross-coupling reactions catalyzed by palladium complexes containing N,N,O-tridentate ligands, Tetrahedron 65 (2009) 2889–2897.

[37] N. Sheng, Chlorido [2-methoxy-6-(2-pyridylmethyliminomethyl)phenolato]zinc(II), Acta Crystallogr. E65 (2009) m1295.

[38] M. Sarwar, A.M. Madalan, C. Tiseanu, G. Novitchi, C. Maxim, G. Marinescu, D. Luneau, M. Andruh, A new synthetic route towards binuclear 3d-4f complexes, using non-compartmental ligands derived from o-vanillin. Syntheses, crystal structures, magnetic and luminescent properties, New J. Chem. 37 (2013) 2280–2292.

[39] R.-H. Hui, P. Zhou, Z.-L. You, Crystal structures of two dinuclear cadmium(II) complexes with Schiff bases as ligands, J. Struct. Chem. 51 (2010) 1201–1204.

[40] Q. Bao, X. Chen, R. Rong, F. Shi, (Dimethylformamide-κO)[2-methoxy-6-(2-pyridylmethyliminomethyl)phenolato-κ³(N,N′,O¹)](thiocyanato-κN)copper(II), Acta Crystallogr. E66 (2010) m563.

[41] S.T. Tsantis, D.I. Tzimopoulos, M. Holynska, S.P. Perlepes, Oligonuclear actinoid complexes with Schiff bases as ligands—older achievements and recent progress, Int. J. Mol. Sci. 21 (2020) 49, article 555 (review).

[42] S.T. Tsantis, V. Bekiari, C.P. Raptopoulou, D.I. Tzimopoulos, V. Psycharis, S.P. Perlepes, Dioxidouranium(VI) complexes with Schiff bases possessing an ONO donor set: synthetic, structural and spectroscopic studies, Polyhedron 152 (2018) 172–178.

[43] S.T. Tsantis, A. Lagou-Rekka, K.F. Konidaris, C.P. Raptopoulou, V. Bekiari, V. Psycharis, S.P. Perlepes, Tetranuclear oxido-bridged thorium(IV) clusters obtained using tridentate Schiff bases, Dalton Trans. 48 (2019) 15668–15678.

[44] S.T. Tsantis, E. Zagoraiou, A. Savvidou, C.P. Raptopoulou, V. Psycharis, L. Szyrwiel, M. Hołyńska, S.P. Perlepes, Binding of oxime group to uranyl ion, Dalton Trans. 45 (2016) 9307–9319.

[45] S.T. Tsantis, M. Mouzakitis, A. Savvidou, C.P. Raptopoulou, V. Psycharis, S.P. Perlepes, The "periodic table" of benzotriazoles: uranium(VI) complexes, Inorg. Chem. Commun. 59 (2015) 57–60.

[46] S.T. Tsantis, P. Danelli, D.I. Tzimopoulos, C.P. Raptopoulou, V. Psycharis, S.P. Perlepes, Pentanuclear thorium(IV) coordination cluster from the use of di(2-pyridyl) ketone, Inorg. Chem. 60 (2021) 11888–11892.

[47] M.S.C. Rigaku, CrystalClear, The Woodlands, TX, USA, 2005.

[48] G.M. Sheldrick, A short history of SHELX, Acta Crystallogr. A64 (2008) 112–122.

[49] G.M. Sheldrick, Crystal structure refinement with SHELXL, Acta Crystallogr. C71 (2015) 3–8.

[50] Diamond, Crystal and Molecular Structure Visualization, Crystal Impact, GbR, Bonn, Germany, 2018. Ver. 3.1.

[51] R.A. Coxall, S.G. Harris, D.K. Henderson, S. Parsons, P.A. Tasker, R.E.P. Winpenny, Inter-ligand reactions: in situ formation of new polydentate ligands, J. Chem. Soc. Dalton Trans. (2000) 2349–2356.

[52] T.W. Hayton, Understanding the origins of O_{yl}–U–O_{yl} bending in the uranyl (UO_2^{2+}) ion, Dalton Trans. 47 (2018) 1003–1009.

[53] M.A. Silver, W.L. Dorfner, S.K. Cary, J.N. Cross, J. Lin, E.J. Schelter, T.E. Albrecht-Schmitt, Why is uranyl formohydroxamate red? Inorg. Chem. 54 (2015) 5280–5284.

[54] K.P. Carter, M. Kalaj, A. Kerridge, J.A. Ridenour, C.L. Cahill, How to bend the uranyl cation via crystal engineering, Inorg. Chem. 57 (2018) 2714–2723.

[55] K. Nakamoto, Infrared and Raman Spectra of Inorganic and Coordination Compounds, fourth ed., Wiley, New York, USA, 1986, pp. 111–113.

[56] J.I. Bullock, Raman and infrared spectroscopic studies of the uranyl ion: the symmetric stretching frequency, force constants, and bond lengths, J. Chem. Soc. A (1969) 781–784.

[57] W.J. Geary, The use of conductivity measurements in organic solvents for the characterization of coordination compounds, Coord. Chem. Rev. 7 (1971) 81–122.

[58] J.M. Harrowfield, B.W. Skelton, A.H. White, Dimethylsuphoxide and its roles in the coordination chemistry of the uranyl ion, C.R. Chim. 8 (2005) 169–180.

[59] C.K. Jørgensen, R. Reisfeld, The uranyl ion, fluorescent and fluorine-like: a review, J. Electrochem. Soc. 130 (1983) 681–684.

[60] P.O. Adelani, P.C. Burns, One-dimensional uranyl-2,2-bipyridine coordination polymer with cation-cation interactions: $(UO_2)_2(2,2'-bpy)(CH_3CO_2)(O)(OH)$, Inorg. Chem. 51 (2012) 11177–11183.

[61] A.F. Leung, L. Hayashibara, J. Spadaro, Fluorescence properties of uranyl nitrates, J. Phys. Chem. Solid. 60 (1999) 299–304.